PTEP

Prog. Theor. Exp. Phys. **2023** 013B01(17 pages)
DOI: 10.1093/ptep/ptac159

IYBSSD2022
International Year
of Basic Sciences
for Sustainable Development

A comprehensive study of the vector leptoquark with $U(1)_{B_3-L_2}$ on the B-meson and muon $g-2$ anomalies

Kayoung Ban[1], Yongsoo Jho[2], Youngjoon Kwon[1], Seong Chan Park[1,⋆], Seokhee Park[3], and Po-Yan Tseng[4]

[1] *Department of Physics and IPAP, Yonsei University, Seoul 03722, Republic of Korea*
[2] *Weizmann Institute, Department of Particle Physics and Astrophysics, Rehovot 7610001, Israel*
[3] *High Energy Accelerator Research Organization (KEK), Tsukuba 305-0801, Japan*
[4] *Department of Physics, National Tsing Hua University, Hsinchu 300, Taiwan*
⋆E-mail: sc.park@yonsei.ac.kr

Received September 1, 2022; Revised November 24, 2022; Accepted November 25, 2022; Published November 28, 2022

Recently reported anomalies in various B-meson decays and also in the anomalous magnetic moment of muon $(g-2)_\mu$ motivate us to consider a particular extension of the standard model incorporating new interactions in the lepton and quark sectors simultaneously. Our minimal choice would be the leptoquark. In particular, we take the vector leptoquark (U_1) and comprehensively study all related observables including $(g-2)_\mu$, $R_{K^{(*)}}$, $R_{D^{(*)}}$, $B \to (K)\ell\ell'$, where $\ell\ell'$ are various combinations of μ and τ, and also lepton flavor violation in the τ decays. We find that a hybrid scenario with an additional $U(1)_{B_3-L_2}$ gauge boson provides a common explanation for all these anomalies.

Subject Index B40, B46, B51, B56

1. Introduction

Physics is a data-driven science, and we are keen to modify the standard model (SM) when experimental results deviate from the theoretical predictions. Over the past several years, the B-physics experiments BaBar, Belle, and LHCb have reported several anomalous results in the $b \to s\ell\ell$ and $b \to c\ell\nu$ processes, which are not properly explained within the SM and thus call for new physics. In particular, the lepton flavor universality (LFU), which is one of the approximate symmetries in the SM, seems to be broken beyond the expected range according to the observables of R_D, R_{D^*}, R_K, and R_{K^*}, which measure the ratios of different lepton flavors:

$$R_{D^{(*)}} \equiv \frac{\mathcal{B}(B \to D^{(*)}\tau\nu)}{\mathcal{B}(B \to D^{(*)}\ell\nu)}, \; R_{K^{(*)}} \equiv \frac{\mathcal{B}(B \to K^{(*)}\mu^+\mu^-)}{\mathcal{B}(B \to K^{(*)}e^+e^-)}. \tag{1}$$

Precise measurement of these quantities would test the basic structure of the SM since LFU is only violated by the lepton masses in the SM.

Funded by SCOAP[3]. SCOAP3 and OUP support the goals of the International Year of Basic Sciences for Sustainable Development

The world averaged experimental values [1] based on measurements from BaBar [2], Belle [3–5], and LHCb [6,7] are

$$R_D = 0.340 \pm 0.027 \pm 0.013 \qquad R_{D^*} = 0.295 \pm 0.011 \pm 0.008\,, \tag{2}$$

and the combined discrepancy with the SM prediction is at the 3.1σ level [1,8].

The most precise measurement to date of R_K has been performed by LHCb [9],

$$R_K = 0.846^{+0.044}_{-0.041}\,, \quad q^2 \subseteq [1.1, 6.0]\ \text{GeV}^2\,, \tag{3}$$

which has a 3.1σ deviation from the SM expectation. For R_{K^*}, LHCb Run-1 provides [10]

$$R_{K^*} = \begin{cases} 0.66^{+0.11}_{-0.07} \pm 0.03\,, & q^2 \subseteq [0.045, 1.1]\ \text{GeV}^2\,, \\ 0.69^{+0.11}_{-0.07} \pm 0.05\,, & q^2 \subseteq [1.1, 6.0]\ \text{GeV}^2\,. \end{cases} \tag{4}$$

Combining both q^2 bins, it has 2.5σ tension with the SM. On the other side, the R_{K^*} and R_K measurements from Belle [11,12],

$$R_{K^*} = \begin{cases} 0.90^{+0.27}_{-0.21} \pm 0.10\,, & q^2 \subseteq [0.1, 8.0]\ \text{GeV}^2\,, \\ 1.18^{+0.52}_{-0.32} \pm 0.10\,, & q^2 \subseteq [15, 19]\ \text{GeV}^2\,, \end{cases}$$

$$R_K = \begin{cases} 0.98^{+0.27}_{-0.23} \pm 0.06\,, & q^2 \subseteq [1.0, 6.0]\ \text{GeV}^2\,, \\ 1.11^{+0.29}_{-0.26} \pm 0.07\,, & 14.18\ \text{GeV} < q^2\,, \end{cases} \tag{5}$$

are still compatible with SM predictions within their large uncertainties. In the near future, Belle II is expected to significantly improve the uncertainties [13].

The other long-standing problem is the anomalous magnetic moment of the muon. Recently, the muon $(g-2)$ experiment at Fermilab reported the value $a_\mu^{\text{FNAL}} = (116\,592\,040 \pm 54) \times 10^{-11}$ [14], or the discrepancy from the SM

$$\Delta a_\mu^{\text{FNAL}} = a_\mu^{\text{FNAL}} - a_\mu^{\text{SM}} = (230 \pm 69) \times 10^{-11}\,, \tag{6}$$

which is a 3.3σ deviation. Since the value is compatible with the earlier value from BNL [15,16], the significance is now strengthened to the 4.2σ level:

$$\Delta a_\mu^{\text{BNL+FNAL}} = a_\mu^{\text{exp}} - a_\mu^{\text{SM}} = (251 \pm 59) \times 10^{-11}\,. \tag{7}$$

Even though it is not completely settled by the lattice calculations [17], it is certainly worth considering new physics as its solution.

Finding a common origin of the B-meson and $(g-2)_\mu$ anomalies is non-trivial, but it is appealing from the theoretical point of view.[1] In early attempts [16,30–40], the $U_1 = (3, 1)_{2/3}$ singlet vector leptoquark, in general coupling to both left-handed (LH) and right-handed (RH) SM fermions, as a single mediator accounts for all the low-energy data. Its simultaneous explanations of the $R_{K^{(*)}}$ and $R_{D^{(*)}}$ anomalies only require LH couplings between second- and third-generation quarks and leptons. However, the LH couplings cannot produce a large enough muon magnetic moment for the $(g-2)_\mu$ anomaly.

In this work, we further extend non-zero RH couplings of U_1 such that it substantially enhances the contribution to $(g-2)_\mu$. In addition, we will also consider $U(1)_{B_3-L_2}$ gauge boson (X) [41–43] to improve our fit to the experimental data. We explore the plausible parameter space and search for a common solution to both the B-meson and $(g-2)_\mu$ anomalies.[2]

[1] See Refs. [18–29] for some of the earlier attempts to account for $(g-2)$ and also various anomalies and possible experimental probes.

[2] When we were finishing our paper, we found that a similar idea was considered in Ref. [44]. Unfortunately, however, the authors of that paper have missed some relevant constraints from low-energy experiments. In particular, the experimental $B_s \to \mu\mu$ data conflict with their preferred parameter region.

2. Model

In this section, we set our theoretical model to explain the B anomalies and $(g-2)_\mu$.

2.1. *Vector leptoquark* $U_1 = (3, 1)_{2/3}$

The leptoquark is a natural candidate for new physics linking the quark sector and the lepton sector [16]. In particular, we focus on the $U_1 = (3, 1)_{2/3}$ weak singlet vector leptoquark because it could provide simultaneous explanations for the $R_{K^{(*)}}$ and $R_{D^{(*)}}$ anomalies with its coupling with LH fermions [30–33]. However, the general Lagrangian includes the U_1 couplings to both LH and RH fermions under the SM gauge symmetry. Including the most relevant interactions with the LH couplings to the second and third generations of leptons and quarks and also the RH couplings, we consider the model Lagrangian:

$$\mathcal{L} \supset U_{1\mu} \sum_{i,j=1,2,3} \left[x_L^{ij} \left(\bar{d}_L^i \gamma^\mu e_L^j \right) + \left(V_{\rm CKM} x_L U^*_{\rm PMNS} \right)_{ij} \left(\bar{u}_L^i \gamma_\mu \nu_L^j \right) + x_R^{ij} \left(\bar{d}_R^i \gamma^\mu e_R^j \right) \right] + \text{h.c.} \quad (8)$$

We adopt the real parts of the CKM and PMNS matrices, which are conveniently written as [16]

$$V_{\rm CKM} x_L U^*_{\rm PMNS} = \begin{pmatrix} 0.974 & 0.225 & 0.001 \\ -0.224 & 0.974 & 0.042 \\ 0.009 & -0.041 & 0.999 \end{pmatrix} \begin{pmatrix} x_L^{11} & x_L^{12} & x_L^{13} \\ x_L^{21} & x_L^{22} & x_L^{23} \\ x_L^{31} & x_L^{32} & x_L^{33} \end{pmatrix} \times \begin{pmatrix} 0.821 & 0.551 & -0.150 \\ -0.307 & 0.600 & 0.739 \\ 0.481 & -0.580 & 0.657 \end{pmatrix};$$

the above expression omits the imaginary parts in $V_{\rm CKM}$, but we adopt the full CKM parameterization from Ref. [45] in our numerical computation. The couplings x_L^{ij} to the first-generation leptons and quarks are strongly constrained from $\mu - e$ conversion on nuclei and atomic parity violation on $\mathcal{B}(K \to \pi \nu \bar{\nu})$; therefore we simply set them zero.

The most relevant Wilson coefficients of the effective Lagrangian in $R_{K^{(*)}}$, $R_{D^{(*)}}$, and $\mathcal{B}(B_s \to \mu\mu)$ are $C_9^{\mu\mu} (= -C_{10}^{\mu\mu})$ [30], and they are induced from the LH couplings

$$C_9^{\mu\mu} = -C_{10}^{\mu\mu} = -\frac{\pi v^2}{V_{tb} V_{ts}^* \alpha_{\rm EM}} \frac{x_L^{22} \left(x_L^{32} \right)^*}{m_{U_1}^2}, \quad (9)$$

where $v = 246$ GeV is the vacuum expectation value of the Higgs and $\alpha_{\rm EM}$ is the fine structure constant. From the fit to R_K, R_{K^*}, and $\mathcal{B}(B_s \to \mu\mu)$ data, we find the parameter window for couplings and the mass of U_1 :

$$C_9^{\mu\mu} = -C_{10}^{\mu\mu} \subseteq [-0.85, -0.50] \Rightarrow -\frac{x_L^{22} \left(x_L^{32} \right)^*}{m_{U_1}^2} \subseteq [0.83, 1.41] \times 10^{-3}\ \text{TeV}^{-2}. \quad (10)$$

The interactions from Eq. (8) also give rise to the effective coefficient [30],

$$g_{V_L} = \frac{v^2}{2 m_{U_1}^2} \left(x_L^{b\ell} \right)^* \left[x_L^{b\ell'} + \frac{V_{cs}}{V_{cb}} x_L^{s\ell'} + \frac{V_{cd}}{V_{cb}} x_L^{d\ell'} \right], \quad (11)$$

and contribute to $b \to c \ell \bar{\nu}_{\ell'}$. It becomes one solution for the R_D and R_{D^*} anomalies, and the 1σ region for $b \to c\tau\bar{\nu}_\tau$ requires

$$g_{V_L} \subseteq [0.09, 0.13] \Rightarrow \frac{\left(V_{cs}^{\rm CKM} x_L^{23} + V_{cb}^{\rm CKM} x_L^{33} \right) \left(x_L^{33} \right)^*}{m_{U_1}^2} \subseteq [0.12, 0.18]\ \text{TeV}^{-2}. \quad (12)$$

The RH couplings x_R, combined with x_L^{22} and x_L^{32}, contribute to the Wilson coefficients $(C_S)' = (C_P)'$; thus their magnitudes are bounded by the $B \to K\tau\mu$ and $B_s \to \mu\mu$ data, which hampers the generation of a large enough muon magnetic dipole for the $(g-2)_\mu$ anomaly. Therefore, we are motivated to further extend our model.

2.2. *Vector leptoquark with the $U(1)_{B_3-L_2}$ X boson*

In the following comprehensive analysis, with the preferred parameter region for the $R_{K^{(*)}}$ and $R_{D^{(*)}}$ anomalies, the U_1 leptoquark itself may still not be able to provide a large enough contribution for the $(g-2)_\mu$ anomaly. Therefore, we invoke the additional particle X, the $U(1)_{B_3-L_2}$ gauge boson, to enhance the contribution, which is an alternative plausible candidate for the R_K anomaly and significantly changes the preferred parameter space. We take the most relevant interactions with the X boson in the effective Lagrangian

$$\mathcal{L}_{\text{e}_\smile}^{X} \supseteq -g_X \bar{\mu}\gamma^\alpha \mu X_\alpha - g_X \bar{\nu}_\mu \gamma^\alpha P_L \nu_\mu X_\alpha + \frac{g_X}{3}\bar{\mathbf{u}}_L \gamma^\alpha \begin{pmatrix} 0 & 0 & 0 \\ 0 & 0 & 0 \\ 0 & 0 & 1 \end{pmatrix} \mathbf{u}_L X_\alpha$$
$$+ \frac{g_X}{3}\bar{\mathbf{d}}_L \gamma^\alpha \underbrace{\begin{pmatrix} |V_{td}|^2 & V_{ts}V_{td}^* & V_{tb}V_{td}^* \\ V_{td}V_{ts}^* & |V_{ts}|^2 & V_{tb}V_{ts}^* \\ V_{td}V_{tb}^* & V_{ts}V_{tb}^* & |V_{tb}|^2 \end{pmatrix}}_{=V_{\text{CKM}}^\dagger V_{B_3} V_{\text{CKM}}} \mathbf{d}_L X_\alpha + \frac{1}{2} m_X^2 X^\mu X_\mu \tag{13}$$

where $\mathbf{u}_L^T \equiv (u_L, c_L, t_L)$ and $\mathbf{d}_L^T \equiv (d_L, s_L, b_L)$. Here, we chose the configuration in which the left-handed down-quark mixing contributes the entire CKM matrix to avoid the constraint from D–$\bar{D}$ mixing. We assume that the m_X is induced by a new Higgs mechanism but the additional contribution from the new Higgs can be neglected. The flavor-changing neutral current (FCNC) in down quarks from the X boson contributes to $B \to K\mu\mu$ and $B_s \to \mu\mu$. At the same time, the muon coupling modifies the $(g-2)_\mu$. In the following, we assume that the $U(1)_{B_3-L_2}$ are broken under the energy scale $\mathcal{O}(100)$ GeV, which justifies the non-zero low-energy effective couplings at the $\mathcal{O}(m_b)$ scale in Eq. (8).

3. Low-energy observables

In this section, we summarize the low-energy observables with the U_1 vector leptoquark contributions.

3.1. *$(g-2)_\mu$*

The previous result of the muon $(g-2)$ experiment with the BNL E821 was 3.7σ from the SM. After the FNAL result, the difference between experiment and SM has become [14,46]

$$\Delta a_\mu = a_\mu^{\text{exp}} - a_\mu^{\text{SM}} = (251 \pm 59) \times 10^{-11}\,, \tag{14}$$

which is a deviation of 4.2σ significance from the SM prediction; this enhances the motivation for SM extensions for new couplings with leptons. In this paper, we present the single leptoquark, which is described in Sect. 2.1 to explain not only the $(g-2)_\mu$ anomaly but also the B-meson anomalies.

For the large mass of the U_1 leptoquark, it contributes to the $(g-2)_\mu$ anomaly as[3]

$$\Delta a_\mu = \frac{N_c}{16\pi^2}\sum_i \Bigg[2Q_U\tilde{\kappa}_Y \mathrm{Im}\left(x_L^{i2}\left(x_R^{i2}\right)^*\right)\frac{m_{d_i}m_\mu}{m_{U_1}^2}\left(\ln\left(\frac{\Lambda_{UV}^2}{M_{U1}^2}\right)+\frac{5}{2}\right)$$
$$+ 2\mathrm{Re}\left(x_L^{i2}\left(x_R^{i2}\right)^*\right)\frac{m_{d_i}m_\mu}{m_{U_1}^2}\left(2Q_d + Q_{U_1}\left((1-\kappa_Y)\ln\left(\frac{\Lambda_{UV}^2}{M_{U1}^2}\right)+\frac{1-5\kappa_Y}{2}\right)\right)$$
$$- \left(\left|x_L^{i2}\right|^2+\left|x_R^{i2}\right|^2\right)\frac{m_\mu^2}{m_{U_1}^2}\left(\frac{4}{3}Q_d + Q_{U_1}\left((1-\kappa_Y)\ln\left(\frac{\Lambda_{UV}^2}{M_{U1}^2}\right)-\frac{1+9\kappa_Y}{6}\right)\right)\Bigg]. \quad (15)$$

If $\kappa_Y \neq 1$ and $\tilde{\kappa}_Y \neq 0$, the dipole moment exhibits logarithmic dependence on the cut-off scale Λ_{UV} not far above the leptoquark mass. So, the leptoquark contribution to the $(g-2)_\mu$ anomaly becomes

$$\Delta a_\mu = \frac{N_c}{16\pi^2}\sum_i \Bigg[2\mathrm{Re}\left(x_L^{i2}\left(x_R^{i2}\right)^*\right)\frac{m_{d_i}m_\mu}{m_{U_1}^2}\left(2Q_d + Q_{U_1}\left(\frac{1-5\kappa_Y}{2}\right)\right)$$
$$- \left(\left|x_L^{i2}\right|^2+\left|x_R^{i2}\right|^2\right)\frac{m_\mu^2}{m_{U_1}^2}\left(\frac{4}{3}Q_d + Q_{U_1}\left(-\frac{1+9\kappa_Y}{6}\right)\right)\Bigg], \quad (16)$$

where we use $\kappa_Y = 1$, $\tilde{\kappa}_Y = 0$, $N_C = 3$, $Q_b = -1/3$, and $Q_{U_1} = 2/3$. We handle the renomalization group running from the leptoquark scale down to the muon mass by evaluating the quark masses at the $\mathcal{O}$(TeV) scale in Eq. (16), e.g., $m_b(\mathrm{TeV}) \simeq 2.4$ GeV [8].

The X boson also contributes to $(g-2)_\mu$ as [18]

$$\Delta a_\mu^X = \frac{g_X^2}{8\pi^2}\int_0^1 dz \frac{2z(1-z)^2}{(1-z)^2 + z(m_X/m_\mu)^2} \quad (17)$$

$$\simeq \left(3g_X^2/4\pi\right)\left(m_\mu^2/m_X^2\right) \quad \text{when } m_X \gg m_\mu \quad (18)$$

$$\simeq 2.7\times 10^{-11}\times\left(\frac{g_X}{0.01}\right)^2\left(\frac{100\ \mathrm{GeV}}{m_X}\right)^2; \quad (19)$$

thus it is negligible compared to the experimental value for $m_X \simeq 100$ GeV and $g_X \simeq 0.01$. However, with X-boson contributions, the preferred parameter space for B-meson anomalies would move and our fit to the data can be significantly improved, as we will describe below.

3.2. $R_{K^{(*)}}$, $R_{D^{(*)}}$

To explain the experimental result of $R_{K^{(*)}}$, it requires the Wilson coefficients to be

$$\Delta C_9^{\mu\mu}|_{\exp} = -0.40 \pm 0.12\,, \qquad \Delta C_9^{U}|_{\exp} = -0.50 \pm 0.38\,, \quad (20)$$

with correlation -0.5 [32,33,47] between them, and the ratio of the SM predictions and experimental observation is

$$\frac{R_D^{\exp}}{R_D^{\mathrm{SM}}} = 1.14 \pm 0.10\,, \qquad \frac{R_{D^*}^{\exp}}{R_{D^*}^{\mathrm{SM}}} = 1.14 \pm 0.05\,, \quad (21)$$

with correlation -0.37 [33]. For the U_1 leptoquark, the contribution to the Wilson coefficients is [32,33]

[3]We use the same κ and $\tilde{\kappa}$ parameters defined in Ref. [8], which are the tri-gauge boson couplings between the U_1 leptoquarks and B_μ gauge boson from $U(1)_Y$. In Eq. (16), we set $\kappa = 1$ and $\tilde{\kappa} = 0$ in such a way that the dipole moment becomes independent of the logarithmic term and UV theory.

$$\Delta C_9^{\mu\mu} = -\Delta C_{10}^{\mu\mu} = -\frac{4\pi^2}{e^2}\frac{v^2}{m_{U_1}^2}\frac{x_L^{32}\left(x_L^{22}\right)^*}{V_{ts}^* V_{tb}}, \tag{22}$$

$$\Delta C_9^U \simeq -\frac{1}{V_{tb}V_{ts}^*}\frac{2}{3}\frac{v^2}{m_{U_1}^2} x_L^{23}\left(x_L^{33}\right)^* \ln\left(\frac{m_b^2}{m_{U_1}^2}\right), \tag{23}$$

where ΔC_9^U is the lepton-universal contribution to $b \to s\ell\ell$ and originates from the x_L^{23} contributing through a log-enhanced photon penguin diagram [33,40]. Similarly, the U_1 contributions to R_D and R_{D^*} are [33]

$$\frac{R_D}{R_D^{\rm SM}} \simeq \left[1 + \frac{v^2}{m_{U_1}^2}{\rm Re}\left\{\left(x_L^{33} - 1.5\eta_S\left(x_R^{33}\right)^*\right)\frac{\left(V_{cb}x_L^{33} + V_{cs}x_L^{23} + V_{cd}x_L^{13}\right)}{V_{cb}}\right\}\right],$$

$$\frac{R_{D^*}}{R_{D^*}^{\rm SM}} \simeq \left[1 + \frac{v^2}{m_{U_1}^2}{\rm Re}\left\{\left(x_L^{33} - 0.14\eta_S\left(x_R^{33}\right)^*\right)\frac{\left(V_{cb}x_L^{33} + V_{cs}x_L^{23} + V_{cd}x_L^{13}\right)}{V_{cb}}\right\}\right], \tag{24}$$

where $\eta_S \simeq 1.8$ accounts for the running of the scalar operator from $m_{U1} = 4$ TeV to m_b.

The additional correction from the X boson to the $\Delta C_9^{\mu\mu}$ is given as [43]

$$\Delta C_9^X = \left(\frac{g_X^2}{3}V_{tb}V_{ts}^*\right)\left(\frac{36\,{\rm TeV}}{m_X}\right)^2$$
$$\approx -0.18 \times \left(\frac{g_X}{0.01}\right)^2\left(\frac{100\,{\rm GeV}}{m_X}\right)^2 \tag{25}$$

It is important to notice that the negative value from V_{ts} makes it trend toward the experimental value for B-meson anomalies but does not contribute to $(g-2)_\mu$.

3.3. $B_c^- \to \tau^-\overline{\nu}_\tau$, $B^+ \to \tau^+\nu_\tau$

The bounds from observation [48,49] and the SM prediction for $B_c \to \tau\nu$ [8,50] are

$$\mathcal{B}(B_c^- \to \tau^-\bar{\nu}_\tau)_{\rm exp} \le 0.60$$
$$\mathcal{B}(B_c^- \to \tau^-\bar{\nu}_\tau)_{\rm SM} = (2.21 \pm 0.09) \times 10^{-2}. \tag{26}$$

The proportion of experimental value and SM prediction for $B^+ \to \tau^+\nu_\tau$ is [8]

$$\frac{\mathcal{B}(B^+ \to \tau^+\nu_\tau)_{\rm exp}}{\mathcal{B}(B^+ \to \tau^+\nu_\tau)_{\rm SM}} = 1.30 \pm 0.29. \tag{27}$$

The U_1 leptoquark contributions to each obervable are [8]

$$\frac{\mathcal{B}\left(B_c^- \to \tau^-\bar{\nu}_\tau\right)}{\mathcal{B}\left(B_c^- \to \tau^-\bar{\nu}_\tau\right)_{\rm SM}} = \left|1 - \frac{\left(V_{cd}x_L^{13} + V_{cs}x_L^{23} + V_{cb}x_L^{33}\right)}{V_{cb}}\frac{v^2}{m_{U_1}^2}\left(\frac{\left(x_L^{33}\right)^*}{2} + \frac{\left(x_R^{33}\right)^* m_{B_c}^2}{m_\tau\left(m_b + m_c\right)}\right)\right|^2, \tag{28}$$

$$\frac{\mathcal{B}\left(B^+ \to \tau^+\nu_\tau\right)}{\mathcal{B}\left(B^+ \to \tau^+\nu_\tau\right)_{\rm SM}} = \left|1 - \frac{\left(V_{ud}x_L^{13} + V_{us}x_L^{23} + V_{ub}x_L^{33}\right)}{V_{ub}}\frac{v^2}{m_{U_1}^2}\left(\frac{\left(x_L^{33}\right)^*}{2} + \frac{\left(x_R^{33}\right)^* m_{B^\pm}^2}{m_\tau m_b}\right)\right|^2. \tag{29}$$

3.4. $B_s^0 \to \tau^+\tau^-$, $B_s^0 \to \mu^+\mu^-$, $B_s^0 \to \tau^\pm\mu^\mp$, *and* $B^+ \to K^+\tau^+\tau^-$

The experimental value from LHCb [51] and the SM prediction [52] are

$$\mathcal{B}(B_s^0 \to \tau^+\tau^-)_{\rm exp} < 6.8 \times 10^{-3} \text{ at } 95\% \text{ CL}, \tag{30}$$

$$\mathcal{B}(B_s^0 \to \tau^+\tau^-)_{\rm SM} = (7.73 \pm 0.49) \times 10^{-7}\,. \tag{31}$$

The related contribution for the U_1 leptoquark is [8]

$$\begin{aligned}\frac{\mathcal{B}\left(B_s^0 \to \tau^+\tau^-\right)}{\mathcal{B}\left(B_s^0 \to \tau^+\tau^-\right)_{\rm SM}} = \frac{16\pi^4}{e^4\left(C_{10}^{\rm SM}\right)^2}\frac{v^4}{m_{U_1}^4}\frac{m_{B_s}^4}{m_\tau^2 m_b^2}\left|\frac{\left(x_L^{33}\right)^* x_R^{23} - \left(x_R^{33}\right)^* x_L^{23}}{V_{ts}^* V_{tb}}\right|^2\left(1 - \frac{4m_\tau^2}{m_{B_s}^2}\right) \\ + \left|1 + \frac{4\pi^2}{e^2 C_{10}^{\rm SM}}\frac{v^2}{m_{U_1}^2}\left(\frac{\left(x_L^{33}\right)^* x_L^{23} + \left(x_R^{33}\right)^* x_R^{23}}{V_{ts}^* V_{tb}}\right.\right. \\ \left.\left. - \frac{m_{B_s}^2}{m_\tau m_b}\frac{\left(x_L^{33}\right)^* x_R^{23} + \left(x_R^{33}\right)^* x_L^{23}}{V_{ts}^* V_{tb}}\right)\right|^2,\end{aligned} \tag{32}$$

where $C_{10}^{\rm SM} \simeq -4.1$, which we use for normalization such that the SM value for the Wilson coefficient matches [53].

The ratio between the SM prediction and experimental value is [8,32]

$$\frac{\mathcal{B}(B_s^0 \to \mu^+\mu^-)_{\rm exp}}{\mathcal{B}(B_s^0 \to \mu^+\mu^-)_{\rm SM}} = 0.73^{+0.13}_{-0.10}\,. \tag{33}$$

The following U_1 vector leptoquark and X-boson total contribution is given by [8,54]

$$\begin{aligned}\frac{\mathcal{B}\left(B_s^0 \to \mu^+\mu^-\right)}{\mathcal{B}\left(B_s^0 \to \mu^+\mu^-\right)_{\rm SM}} = \frac{16\pi^4}{e^4\left(C_{10}^{\rm SM}\right)^2}\frac{v^4}{m_{U_1}^4}\frac{m_{B_s}^4}{m_\mu^2 m_b^2}\left|\frac{\left(x_L^{32}\right)^* x_R^{22} - \left(x_R^{32}\right)^* x_L^{22}}{V_{ts}^* V_{tb}}\right|^2 \\ + \left|1 + \frac{4\pi^2}{e^2 C_{10}^{\rm SM}}\frac{v^2}{m_{U_1}^2}\left(\frac{\left(x_L^{32}\right)^* x_L^{22} + \left(x_R^{32}\right)^* x_R^{22}}{V_{ts}^* V_{tb}}\right.\right. \\ \left. - \frac{m_{B_s}^2}{m_\mu m_b}\frac{\left(x_L^{32}\right)^* x_R^{22} + \left(x_R^{32}\right)^* x_L^{22}}{V_{ts}^* V_{tb}}\right) \\ \left. - \left[\frac{\alpha}{2\pi\sin^2\theta_W}Y\left(\frac{m_t^2}{m_W^2}\right)\right]^{-1}\left(\frac{2\,g_X^2\,m_Z^2}{3\,g^2\,m_X^2}\right)\right|^2,\end{aligned} \tag{34}$$

where the last term in the second absolute bracket comes from the X boson. Here we take $Y(m_t^2/m_W^2) = 1.05$, and $g \simeq 0.652$ the $SU(2)_L$ coupling constant.

The LHCb search on $B_s^0 \to \tau^\pm\mu^\mp$ provides an upper limit,

$$\mathcal{B}(B_s^0 \to \tau^\pm\mu^\mp)_{\rm exp} < 2.1 \times 10^{-5}, \tag{35}$$

at the 95% confidence level [55]. The SM prediction of this branching fraction is extremely small, $\mathcal{O}(10^{-54})$ [56]. The expression for the U_1 contribution to $B_s^0 \to \tau^\pm\mu^\mp$ is [33]

$$\begin{aligned}\mathcal{B}\left(B_s^0 \to \tau^\pm\mu^\mp\right) = \frac{1}{\Gamma_{B_s}}\frac{m_{B_s} f_{B_s}^2 G_F^2}{8\pi}m_\tau^2\left(1 - \frac{m_\tau^2}{m_{B_s}^2}\right)^2 \\ \times \frac{v^4}{4m_{U_1}^4}\left|x_L^{22}\left(x_L^{33}\right)^* - \frac{2\eta_S m_{B_s}^2}{m_\tau\left(m_s + m_b\right)}x_L^{22}\left(x_R^{33}\right)^*\right|^2,\end{aligned} \tag{36}$$

where $G_F = 1.166 \times 10^{-5}$ GeV^{-2} is the Fermi constant, $f_{B_s} = 0.225$ GeV [57] is the leptonic decay constant of B_s^0, and $\Gamma_{B_s} = 4.34 \times 10^{-13}$ GeV is the total width of B_s^0.

The BaBar experiment measured the branching fraction [58]

$$\mathcal{B}(B^+ \to K^+\tau^+\tau^-)_{\rm exp} = (1.31 \pm 0.71) \times 10^{-3} \tag{37}$$

with an upper limit of $\mathrm{Br}(B^+ \to K^+\tau^+\tau^-) < 2.25 \times 10^{-3}$ at the 90% confidence level. The expression for the U_1 leptoquark contribution to this process is given by [33]

$$\mathcal{B}\left(B^+ \to K^+\tau^+\tau^-\right) \simeq 1.5 \times 10^{-7} + 10^{-3}\frac{v^2}{2m_{U_1}^2}\left[1.4\,\mathrm{Re}\left(x_L^{23}\left(x_L^{33}\right)^*\right) - 3.3\,\mathrm{Re}\left(x_L^{23}\left(x_R^{33}\right)^*\right)\right] + \frac{v^4}{4m_{U_1}^4}\left|x_L^{23}\right|^2\left[3.5\left|x_L^{33}\right|^2 - 16.4\,\mathrm{Re}\left(x_R^{33}\left(x_L^{33}\right)^*\right) + 95.0\left|x_R^{33}\right|^2\right], \quad (38)$$

where $v = 246$ GeV is the electroweak vacuum expectation value.

3.5. $B^+ \to K^+\tau^+\mu^-$, $B^+ \to K^+\tau^-\mu^+$

From the BaBar experiment, we obtain upper limits [59]

$$\mathcal{B}(B^+ \to K^+\tau^+\mu^-) < 2.8 \times 10^{-5}, \quad (39)$$

$$\mathcal{B}(B^+ \to K^+\tau^-\mu^+) < 4.5 \times 10^{-5} \quad (40)$$

at the 90% confidence level. The leptoquark contribution is given by [33,60]

$$\mathcal{B}\left(B^+ \to K^+\tau^+\mu^-\right) \simeq \frac{v^4}{4m_{U_1}^4}\left|x_L^{22}\right|^2\left[8.3\left|x_L^{33}\right|^2 + 155.2\left|x_R^{33}\right|^2 - 42.3\,\mathrm{Re}\left(\left(x_L^{33}\right)^* x_R^{33}\right)\right],$$
$$\mathcal{B}\left(B^+ \to K^+\tau^-\mu^+\right) \simeq 8.3\frac{v^4}{4m_{U_1}^4}\left|x_L^{32}\left(x_L^{23}\right)^*\right|^2. \quad (41)$$

3.6. $\tau \to \mu\gamma$, $\mu\phi$, *and LFU in* τ *decays*

Due to its sizeable couplings to muon and tau leptons, the U_1 leptoquark can significantly affect the lepton flavor violation in τ decays. The experimental upper limits are [61,62]

$$\mathcal{B}(\tau \to \mu\gamma) < 3.0 \times 10^{-8} \quad (42)$$

$$\mathcal{B}(\tau \to \mu\phi) < 5.1 \times 10^{-8} \quad (43)$$

at the 90% confidence level. In addition, the LFU in the decay of charged leptons can give stringent bounds on the leptoquark couplings. The experimentally measured values are [61,63]

$$(g_\tau/g_\mu)_{\mathrm{exp}} = 1.0000 \pm 0.0014, \quad (44)$$

$$(g_\tau/g_\mu)_\ell = 1.0010 \pm 0.0015, \quad (45)$$

$$(g_\tau/g_\mu)_\pi = 0.9961 \pm 0.0027, \quad (46)$$

$$(g_\tau/g_\mu)_K = 0.9860 \pm 0.0070. \quad (47)$$

For the U_1 leptoquark contribution to $\mathcal{B}(\tau \to \mu\gamma)$, we adopt a complete formula of the decay width [64],

$$\Gamma(\tau \to \mu\gamma) = \frac{\alpha_{\mathrm{EM}}\left(m_\tau^2 - m_\mu^2\right)^3}{4m_\tau^3}\left(\left|\sigma_L^{32}\right|^2 + \left|\sigma_R^{32}\right|^2\right), \quad (48)$$

where

$$\sigma_L^{32} = -\frac{iN_c}{16\pi^2 m_{U_1}^2} \sum_{k=1,2,3} \left\{ \frac{2}{3} \left[\left(x_R^{k2*} x_R^{k3} m_\tau + x_L^{k2*} x_L^{k3} m_\mu \right) g(t_k) + x_R^{k2*} x_L^{k3} m_{d_k} j(t_k) \right] - \frac{1}{3} \left[\left(x_R^{k2*} x_R^{k3} m_\tau + x_L^{k2*} x_L^{k3} m_\mu \right) f(t_k) + x_R^{k2*} x_L^{k3} m_{d_k} h(t_k) \right] \right\}$$

$$\sigma_R^{32} = -\frac{iN_c}{16\pi^2 m_{U_1}^2} \sum_{k=1,2,3} \left\{ \frac{2}{3} \left[\left(x_L^{k2*} x_L^{k3} m_\tau + x_R^{k2*} x_R^{k3} m_\mu \right) g(t_k) + x_L^{k2*} x_R^{k3} m_{d_k} j(t_k) \right] - \frac{1}{3} \left[\left(x_L^{k2*} x_L^{k3} m_\tau + x_R^{k2*} x_R^{k3} m_\mu \right) f(t_k) + x_L^{k2*} x_R^{k3} m_{d_k} h(t_k) \right] \right\} \quad (49)$$

with $t_k \equiv m_{d_k}^2 / m_{U_1}^2$ and f, g, h, j are loop functions [64].

For $\mathcal{B}(\tau \to \mu\phi)$, it is given by [33,65]

$$\mathcal{B}(\tau \to \mu\phi) = \frac{1}{\Gamma_\tau} \frac{f_\phi^2 G_F^2}{16\pi} m_\tau^3 \left(1 - \frac{m_\phi^2}{m_\tau^2}\right)^2 \left(1 + \frac{2m_\phi^2}{m_\tau^2}\right) \frac{v^4}{4m_{U_1}^4} \left| x_L^{23} \left(x_L^{22}\right)^* \right|^2 , \quad (50)$$

where ϕ is the $s\bar{s}$ vector meson with $f_\phi = 0.225$ GeV, $m_\phi = 1.019$ GeV [65]. For LFU in lepton decays, we use the expression [33,63]

$$\left(\frac{g_\tau}{g_\mu}\right)_{\ell,\pi,K} \simeq 1 - 0.08 \times \frac{\left(x_L^{33}\right)^2 v^2}{4m_{U1}^2} . \quad (51)$$

More specifically, they can be written in terms of the effective Lagrangian for leptonic decay [63],

$$\mathcal{L}_{\ell \to \ell' \nu \bar{\nu}} = -\frac{4G_F}{\sqrt{2}} \left(\left[C_{\nu e}^{\mathrm{V,LL}}\right]_{\rho\sigma\alpha\beta} \left(\bar{\nu}_L^\rho \gamma^\mu \nu_L^\sigma\right) \left(\bar{\ell}_L^\alpha \gamma^\mu \ell_L^\beta\right) + \left[C_{\nu e}^{\mathrm{V,LR}}\right]_{\rho\sigma\alpha\beta} \left(\bar{\nu}_L^\rho \gamma^\mu \nu_L^\sigma\right) \left(\bar{\ell}_R^\alpha \gamma^\mu \ell_R^\beta\right) \right) , \quad (52)$$

and, for hadronic decay [63],

$$\mathcal{L}_{\tau \to h\nu} = -\frac{4G_F}{\sqrt{2}} \sum_\rho \left\{ \left(\delta_{\rho 3} \left(V_{\mathrm{CKM}}\right)_{ji}^* \left[C_{\nu edu}^{\mathrm{V,LL}}\right]_{\rho 3ij} \right) \left(\bar{\nu}_L^\rho \gamma^\mu \tau_L\right) \left(\bar{d}_L^i \gamma^\mu u_L^j\right) + \left[C_{\nu edu}^{\mathrm{S,RL}}\right]_{\rho 3ij} \left(\bar{\nu}_L^\rho \tau_L\right) \left(\bar{d}_R^i u_R^j\right) \right\} , \quad (53)$$

resulting in the following expressions for couplings with τ and μ:

$$\left(\frac{g_\tau}{g_\mu}\right)_\ell = \left[\frac{\sum_{\rho\sigma}\left(\left|\delta_{\rho3}\delta_{\sigma1} + \left[C_{\nu e}^{\mathrm{V,LL}}\right]_{\rho\sigma13}\right|^2 + \left|\left[C_{\nu e}^{\mathrm{V,LR}}\right]_{\rho\sigma13}\right|^2\right)}{\sum_{\rho\sigma}\left(\left|\delta_{\rho2}\delta_{\sigma1} + \left[C_{\nu e}^{\mathrm{V,LL}}\right]_{\rho\sigma12}\right|^2 + \left|\left[C_{\nu e}^{\mathrm{V,LR}}\right]_{\rho\sigma12}\right|^2\right)}\right]^{1/2},$$

$$\left(\frac{g_\tau}{g_\mu}\right)_\pi = \left(\frac{\sum_\rho\left|\delta_{\rho3}V_{ud}^* + \left[C_{\nu edu}^{\mathrm{V,LL}}\right]_{\rho311} + \frac{m_\pi^2}{m_\tau(m_d+m_u)}\left[C_{\nu edu}^{\mathrm{S,RL}}\right]_{\rho311}\right|^2}{\sum_\rho\left|\delta_{\rho2}V_{ud} + \left[C_{\nu edu}^{\mathrm{V,LL}}\right]_{\rho211}^* + \frac{m_\pi^2}{m_\mu(m_d+m_u)}\left[C_{\nu edu}^{\mathrm{S,RL}}\right]_{\rho211}^*\right|^2}\right)^{1/2},$$

$$\left(\frac{g_\tau}{g_\mu}\right)_K = \left(\frac{\sum_\rho\left|\delta_{\rho3}V_{us}^* + \left[C_{\nu edu}^{\mathrm{V,LL}}\right]_{\rho321} + \frac{m_K^2}{m_\tau(m_d+m_u)}\left[C_{\nu edu}^{\mathrm{S,RL}}\right]_{\rho321}\right|^2}{\sum_\rho\left|\delta_{\rho2}V_{us} + \left[C_{\nu edu}^{\mathrm{V,LL}}\right]_{\rho221}^* + \frac{m_K^2}{m_\mu(m_d+m_u)}\left[C_{\nu edu}^{\mathrm{S,RL}}\right]_{\rho221}^*\right|^2}\right)^{1/2}. \qquad (54)$$

For the U_1 leptoquark, by using the Fierz transformation in Eq. (8),

$$[\bar{u}_{1L}\gamma^\mu u_{2L}][\bar{u}_{3L}\gamma_\mu u_{4L}] = -[\bar{u}_{1L}\gamma^\mu u_{4L}][\bar{u}_{3L}\gamma_\mu u_{2L}],$$

we replace the Wilson coefficients as

$$\left[C_{\nu edu}^{\mathrm{V,LL}}\right]_{\rho\sigma ij} \Leftrightarrow -\frac{2v^2}{4m_{U_1}^2}\left(V_{\mathrm{CKM}}x_L U_{\mathrm{PMNS}}^*\right)_{j\rho}(x_L)_{i\sigma},$$
$$\left[C_{\nu edu}^{\mathrm{S,RL}}\right] = \left[C_{\nu e}^{\mathrm{V,LL}}\right] = \left[C_{\nu e}^{\mathrm{V,LR}}\right] = 0. \qquad (55)$$

4. Parameter scanning

We perform χ^2 parameter scanning, with the values of all 17 observables constituting the χ^2 listed in Table 1, which includes anomalies of $R_{K^{(*)}}$, $R_{D^{(*)}}$, constraints from other B-meson decay channels, and constraints from τ decays. Under the null hypothesis (SM only), we have $\chi^2_{\mathrm{SM}} = 26.0$ along with $p_{\mathrm{SM}} = 0.074$, where p_{SM} is the P-value of the null hypothesis. We compare this result with the following three scenarios:

- **Scan-1**: $P_{\text{scan-1}} = (x_L^{22}, x_L^{23}, x_L^{32}, x_L^{33})$, with $m_{U_1} = 2.5$ TeV.
  Results are shown in Fig. 1.
- **Scan-2**: $P_{\text{scan-2}} = P_{\text{scan-1}} \oplus x_R^{32}$, with $m_{U_1} = 2$ TeV.
  Results are shown in Fig. 2.
- **Scan-3**: $P_{\text{scan-3}} = P_{\text{scan-2}} \oplus g_X$, with $m_{U_1} = 2$ TeV and $m_X = 100$ GeV.
  Results are shown in Fig. 3.

For **scan-1**, we choose a set of relevant couplings, $x_L^{22}, x_L^{23}, x_L^{32}, x_L^{33}$, that is sufficient to explain the B-meson anomalies and satisfies all the low-energy observables. It gives rise to the best-fitting $\chi^2_{\mathrm{min},1} = 9.23$ and $p_1 = 0.755$ with $(x_L^{22}, x_L^{23}, x_L^{32}, x_L^{33}) = (7.90 \times 10^{-2}, 0.328, -3.83 \times 10^{-2}, 0.862)$ and $m_{U_1} = 2$ TeV. Figure 1 shows the 1σ region for **scan-1**. The favored region of the (x_L^{23}, x_L^{33}) plane, shown in the upper-left panel of Fig. 1, is mainly determined by $R_{D^{(*)}}$; meanwhile, $R_{K^{(*)}}$ dictates the favored region of the (x_L^{22}, x_L^{32}) plane. There is a contribution to Δa_μ from the LH couplings, as shown in the upper-right panels of Fig. 1. However, it is not

Table 1. List of observables for the χ^2 scanning with the measured values and predictions from SM. The equations of the $U_1(+X)$ model are also referenced.

Observable	Experiment	SM predict	$U_1(+X)$ predict
$R_{D^{(*)}}$	$\frac{R_D^{\rm exp}}{R_D^{\rm SM}} = 1.14 \pm 0.10$, $\frac{R_{D^*}^{\rm exp}}{R_{D^*}^{\rm SM}} = 1.14 \pm 0.05$		Eq. (24)
$\Delta C_9^{\mu\mu} = -\Delta C_{10}^{\mu\mu}$ $(R_{K^{(*)}})$	-0.40 ± 0.12	0	Eq. (22)
ΔC_9^U	-0.50 ± 0.38	0	Eqs. (23), (25)
$B_c^- \to \tau^-\bar{\nu}_\tau$	≤ 0.60	$(2.21 \pm 0.09) \times 10^{-2}$	Eq. (28)
$B^+ \to \tau^+\nu_\tau$	$(1.09 \pm 0.24) \times 10^{-4}$	$(8.8 \pm 0.6) \times 10^{-5}$	Eq. (29)
$B_s^0 \to \tau^+\tau^-$	$<6.8 \times 10^{-3}$	$(7.73 \pm 0.49) \times 10^{-7}$	Eq. (32)
$B_s^0 \to \mu^+\mu^-$	$\frac{BR(B_s^0 \to \mu^+\mu^-)^{\rm exp}}{BR(B_s^0 \to \mu^+\mu^-)^{\rm SM}} = 0.73^{+0.13}_{-0.10}$		Eq. (34)
$B_s^0 \to \tau^\pm\mu^\mp$	$<2.1 \times 10^{-5}$		Eq. (36)
$B^+ \to K^+\tau^+\tau^-$	$(1.31 \pm 0.71) \times 10^{-3}$	$(1.20 \pm 0.12) \times 10^{-7}$	Eq. (41)
$B^+ \to K^+\tau^+\mu^-$	$\leq 2.8 \times 10^{-5}$		Eq. (41)
$B^+ \to K^+\tau^-\mu^+$	$\leq 4.5 \times 10^{-5}$		Eq. (41)
$\tau \to \mu\gamma$	$<3.0 \times 10^{-8}$		Eq. (48)
$\tau \to \mu\phi$	$<5.1 \times 10^{-8}$		Eq. (50)
LFU in τ decay	$(g_\tau/g_\mu)_\ell = 1.0010 \pm 0.0015$		Eq. (54)
	$(g_\tau/g_\mu)_\pi = 0.9961 \pm 0.0027$		
	$(g_\tau/g_\mu)_K = 0.9860 \pm 0.0070$		

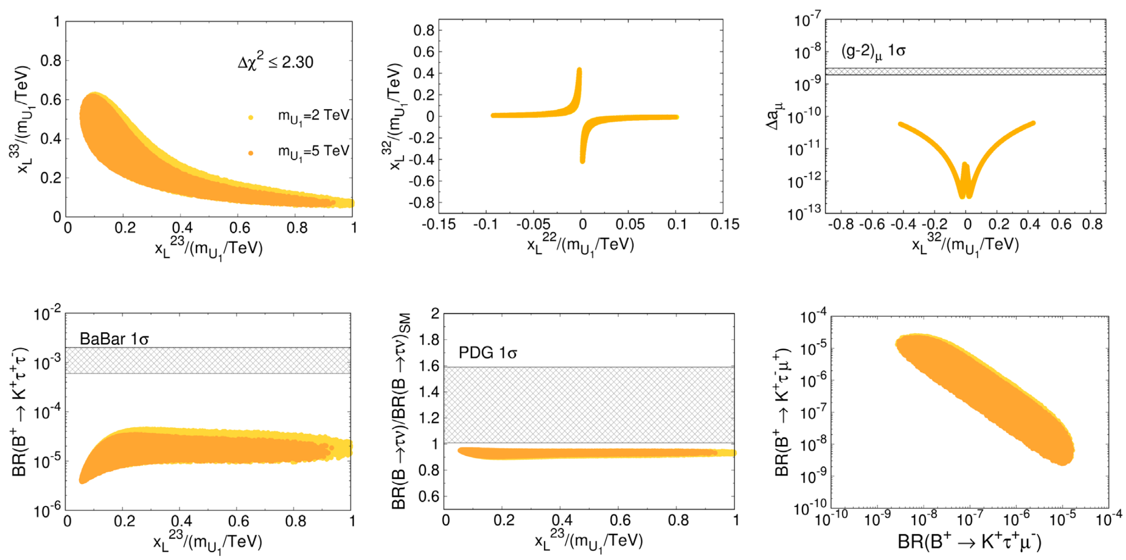

Fig. 1. Scan-1: The region satisfies $\Delta\chi^2 \equiv \chi^2 - \chi^2_{\rm min,1} \leq 2.3$, and $\chi^2_{\rm min,1} = 9.23$.

large enough to explain the recent measurement from Fermilab, thus providing the motivation to turn on the RH coupling in **scan-2**.

In **scan-2** ($\chi^2_{\rm min,2} = 9.06$ and $p_2 = 0.698$), according to Eq. (16), we found that the most efficient way to enhance Δa_μ is to use x_R^{32}, due to the fact that the multiplicity of $(x_L^{32} x_R^{32})$ has a weaker mass suppression factor $(m_b m_\mu / m_{U_1})$ than that of pure LH couplings or RH couplings. In the $(x_L^{32}, \Delta a_\mu)$ and $(x_R^{32}, \Delta a_\mu)$ planes of Fig. 2, they show that the value of Δa_μ can be increased by more than an order of magnitude in contrast to **scan-1**. However, it still cannot explain the BNL and FNAL results without an additional contribution. For example, incorpo-

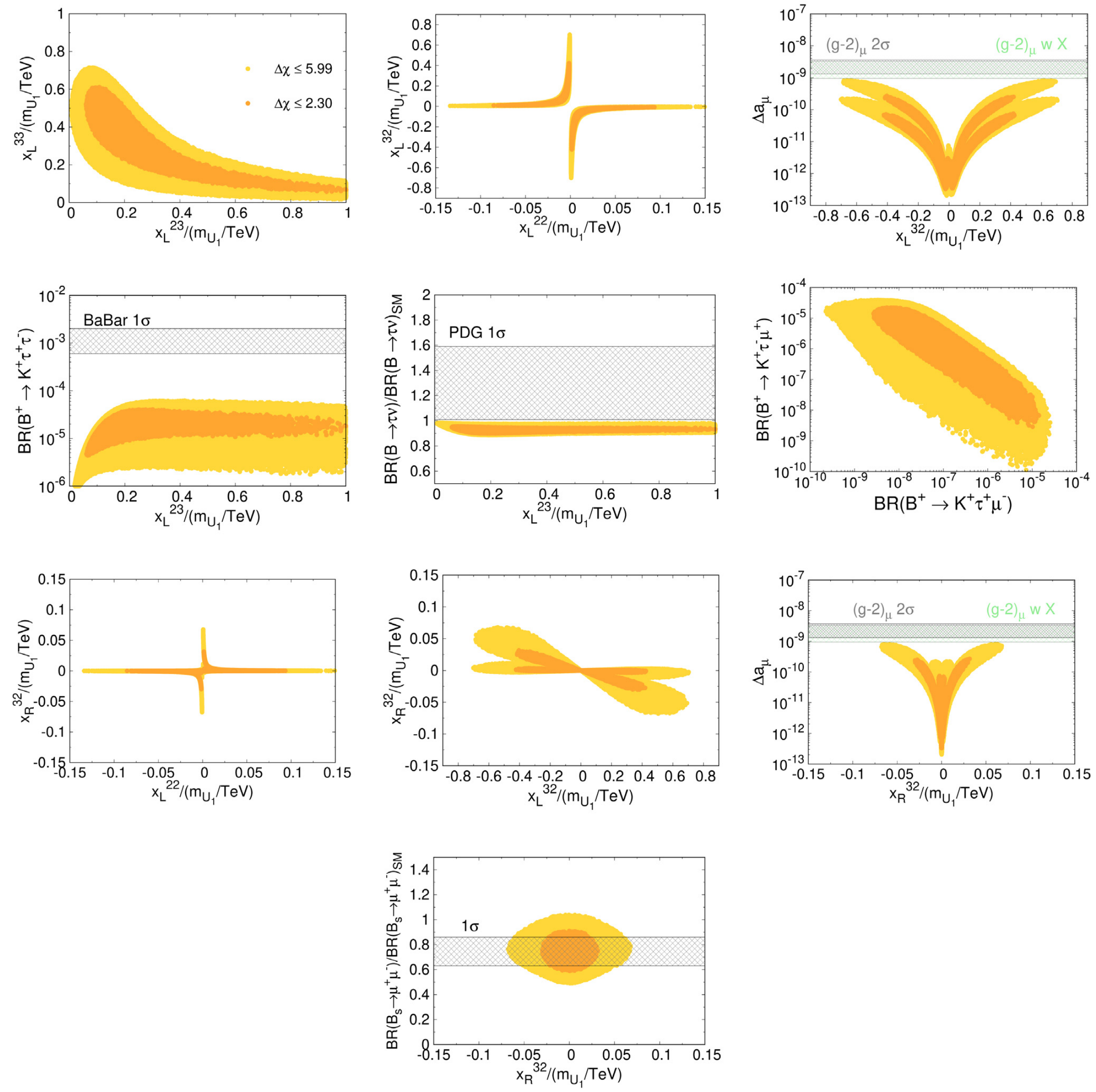

Fig. 2. Scan-2: The 1σ (2σ) region satisfies $\Delta\chi^2 \equiv \chi^2 - \chi^2_{\min,2} \leq 2.30$ (5.99), and $\chi^2_{\min,2} = 9.06$. Here we fix $m_{U_1} = 2$ TeV. The green hatched regions show the effect of a muon-philic X vector boson with coupling $g_X = 0.2$ and mass $m_X = 100$ GeV, which gives $\Delta a_\mu|_X = 38 \times 10^{-11}$.

rating a muon-philic vector boson X with coupling $g_X = 0.2$ and mass $m_X = 100$ GeV, which is consistent with current experimental bounds, gives $\Delta a_\mu|_X = 38 \times 10^{-11}$, shown by the green hatched regions overlapping with the U_1 2σ-allowed region in Fig. 2.

In **scan-3**, we include a specific $U(1)_{B_3-L_2}$ X boson in addition to the U_1 leptoquark framework, and demonstrate that under this framework it can alleviate the $(g-2)_\mu$ and B-physics tensions within 2σ. Not only the $(g-2)_\mu$ but also this X boson contributes to both ΔC_9 (see Eq. (25)) and $B_s \to \mu\mu$ (see Eq. (34)). In particular, we vary the coupling $0.01 \leq g_X \leq 0.05$ and fix $m_X = 100$ GeV, which is partially allowed under current experimental constraints from neutrino-trident [66], $B_s^0 - \bar{B}_s^0$ mixing [67], $K_L \to \mu^+\mu^-$ [68], ATLAS [69], and CMS [70,71].

It is worth mentioning the reliable range of X-boson parameters consistent with the measurement of (i) B_s^0–$\bar{B}_s^0$ mixing (ΔM_s), (ii) $\mathrm{Br}(K_L \to \mu^+\mu^-)$, and (iii) K^0–$\bar{K}^0$ mixing parameters. The mass difference ΔM_s has been precisely measured by the CDF2, LHCb, and CMS col-

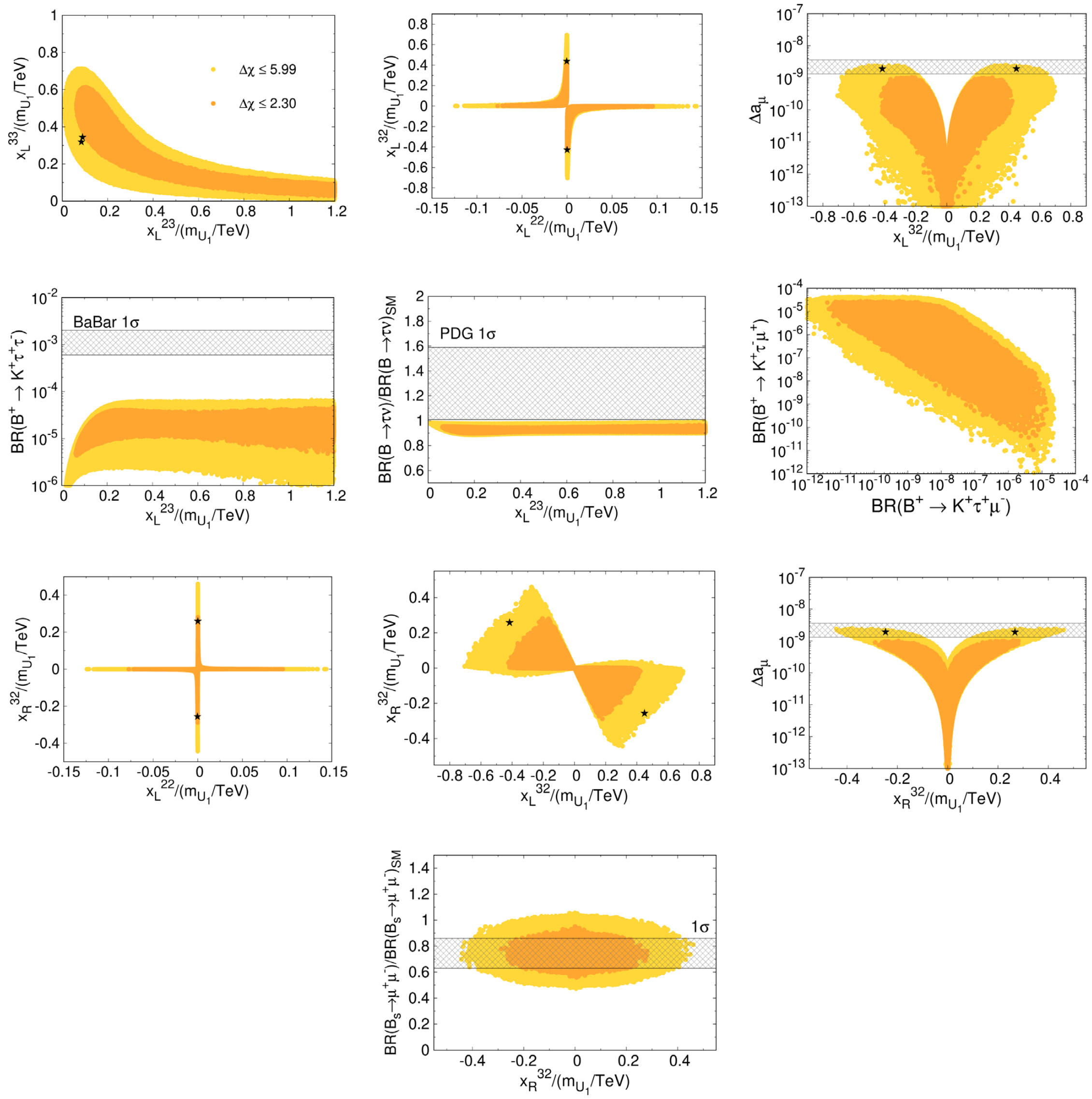

Fig. 3. Scan-3: Same as Fig. 2, but includes the contribution of the additional $U(1)_{B_3-L_2}$ X boson. Here we vary $0.01 \leq g_X \leq 0.05$ and meanwhile fix $m_{U_1} = 2$ TeV and $m_X = 100$ GeV.

laborations [72,73], and its theoretical predictions has been improved by developed sum rules and lattice calculations. We use the weighted average of the latest results given in Ref. [67] as our $\Delta M_s^{\rm SM}$. In the presence of the X boson, the new physics contribution to ΔM_s is approximated by $\frac{\Delta M_s^{\rm SM+NP}}{\Delta M_s^{\rm NP}} \approx \left|1 + \frac{1}{360}\left(\frac{\delta C_9^\mu}{-0.53}\right)^2\left(\frac{m_X/g_X}{1\ \rm TeV}\right)^2\right|$ [67]. Putting $\delta C_9^\mu(= -\delta C_{10}^\mu) = -0.40 \pm 0.12$ [32,33,47] into the expression and requiring $\Delta M_s = (1.04^{+0.04}_{-0.07})\Delta M_s^{\rm exp}$, the lower limit on the coupling is $g_X > 1.01 \times 10^{-2}$ within 1σ for $m_X = 100$ GeV.[4] For $\mathrm{Br}(K_L \to \mu^+\mu^-)$, requiring that the new physics contribution to the dimension-six $\Delta F = 1$ operator $(\bar{s}_L\gamma^\mu d_L)(\bar{\mu}\gamma_\mu\mu)$ is smaller than the SM contribution [68,75], we impose the upper limit on the coupling $g_X < 4.61 \times 10^{-2}$ for $m_X = 100$ GeV. Focusing on the upper limit on the short-distance contribution $\mathrm{Br}(K_L \to \mu^+\mu^-)_{\rm SD}$, a dedicated analysis gives $g_X|_{m_X=100\ \rm GeV} < 3.55 \times 10^{-2}$ [76]. For the neutral kaon

[4]Using the global fit $\delta C_9^\mu(= -\delta C_{10}^\mu) = -0.39 \pm 0.07$ based on the Moriond 2021 result [74], the lower limit on the coupling is $g_X > 1.15 \times 10^{-2}$ within 1σ for $m_X = 100$ GeV.

mixing, the most stringent bound comes from the measurement of ϵ_K. Following the approach in Ref. [76], we get the allowed range on the coupling as $-4.13 \times 10^{-2} < g_X < 4.24 \times 10^{-2}$ for $m_X = 100$ GeV. We assume that the left-handed coupling to the X boson is dominant for flavor-violating vertices in the hadronic sector.

Such an X boson has a negligible effect on $(g-2)_\mu$, but gives a modest contribution to ΔC_9. Due to the negative value of $V_{ts} \simeq -0.40$, the X boson trends to the observed value ($C_9^{\mu\mu} = -0.40 \pm 0.12$). Consequently, the U_1 leptoquark in conjunction with the X boson explains the $R_{K^{(*)}}$ anomaly, but the former solely contributes to $(g-2)_\mu$. Compared to **scan-2**, the $\chi^2_{\rm min} = 9.06$ at $(x_L^{22}, x_L^{23}, x_L^{32}, x_L^{33}, x_R^{32}, g_X) = (4.04 \times 10^{-2}, 0.324, -9.30 \times 10^{-3}, 0.810, 3.73 \times 10^{-4}, 1.47 \times 10^{-2})$ is no further reduced by including the X boson. However, the 2σ chi-squared regions (yellow regions in Fig. 3) extend to overlap with the $(g-2)_\mu$ 2σ region. Two representative points in the overlapping regions are

$$\left(x_L^{22}, x_L^{23}, x_L^{32}, x_L^{33}, x_R^{32}, g_X\right) = \begin{cases} (+3.28 \times 10^{-4}, 0.167, -0.846, 0.644, +0.520, 1.32 \times 10^{-2}), \\ (-3.08 \times 10^{-4}, 0.227, +0.831, 0.668, -0.554, 1.44 \times 10^{-2}), \end{cases}$$

respectively giving $(\chi^2, \Delta a_\mu) = (13.9, 193 \times 10^{-11})$ and $(\chi^2, \Delta a_\mu) = (13.7, 201 \times 10^{-11})$. As a result, this hybrid scenario, the U_1 leptoquark in conjunction with the $U(1)_{B_3-L_2}$ gauge boson, explains the B-physics and $(g-2)_\mu$ anomalies within 2σ.

5. Summary

The recent observational anomalies lead us to consider a vector leptoquark whose couplings with both left and right chiral fermions are essential. It affects various channels of B-meson decays and generates lepton flavor universality breaking. At the same time, the leptoquark can contribute to $(g-2)_\mu$ with significant enhancement. We perform a global analysis of several low-energy observables and encounter both left- and right-handed U_1 leptoquark couplings. Unfortunately, we have not found a common parameter region for the B and $(g-2)_\mu$ anomalies without an additional muon-philic vector boson. Motivated by this, we found that the U_1 leptoquark in conjunction with the additional $U(1)_{B_3-L_2}$ gauge boson is able to reconcile the B-physics and $(g-2)_\mu$ anomalies within 2σ. We expect that the experimental measurements will be much improved in the future and the leptoquark and the new gauge boson will be better tested accordingly.

Acknowledgements

The work is supported by the National Research Foundation of Korea NRF-2021R1A4A2001897, NRF-2019R1A2C1089334 (S.C.P.), and NRF-2020R1I1A1A01066413 (P.Y.T.). We thank Andreas Crivellin for discussions on the bottom-quark mass in the computation of muon $(g-2)$. S.C.P. is grateful to Michael Peskin for the invitation to the symposium on the muon $g-2$ anomaly and discussion. S.C.P. also acknowledges the support from Yonsei U. and KIAS during his sabbatical period. We acknowledge the hospitality of APCTP, where part of this work was done.

Funding

Open Access funding: SCOAP^3.

References

[1] Y. S. Amhis et al., Eur. Phys. J. C **81**:226 (2021) [arXiv:1909.12524] [Search inSPIRE].
[2] J. P. Lees et al., Phys. Rev. Lett. **109**, 101802 (2012) [arXiv:1205.5442] [Search inSPIRE].
[3] M. Huschle et al., Phys. Rev. D **92**, 072014 (2015) [arXiv:1507.03233] [Search inSPIRE].

[4] S. Hirose et al., Phys. Rev. Lett. **118**, 211801 (2017) [arXiv:1612.00529] [Search inSPIRE].
[5] G. Caria et al., Phys. Rev. Lett. **124**, 161803 (2020) [arXiv:1910.05864] [Search inSPIRE].
[6] R. Aaij et al., Phys. Rev. Lett. **115**, 111803 (2015); **115**, 159901 (2015) [erratum][arXiv:1506.08614] [Search inSPIRE].
[7] R. Aaij et al., Phys. Rev. Lett. **120**, 171802 (2018) [arXiv:1708.08856] [Search inSPIRE].
[8] W. Altmannshofer, S. Gori, H. H. Patel, S. Profumo, and D. Tuckler, J. High Energy Phys. **2005**, 069 (2020) [arXiv:2002.01400] [Search inSPIRE].
[9] R. Aaij et al., Nature Physics **18**, 277–282 (2022) [arXiv:2103.11769] [Search inSPIRE].
[10] R. Aaij et al., J. High Energy Phys. **1708**, 055 (2017) [arXiv:1705.05802] [Search inSPIRE].
[11] A. Abdesselam et al., Phys. Rev. Lett. **126**, 161801 (2021)arXiv:1904.02440[Search inSPIRE].
[12] S. Choudhury et al., J. High Energy Phys. **2103**, 105 (2021) [arXiv:1908.01848] [Search inSPIRE].
[13] E. Kou, P. Urquijo, W. Altmannshofer et al., Prog. Theor. Exp. Phys. **2019**, 123C01 (2019).
[14] B. Abi, T. Albahri, S. Al-Kilani et al., Phys. Rev. Lett. **126**, 141801 (2021).
[15] G. W. Bennett et al., Phys. Rev. D **73**, 072003 (2006) [arXiv:hep-ex/0602035] [Search inSPIRE].
[16] P. A. Zyla et al., Prog. Theor. Exp. Phys. **2020**, 083C01 (2020).
[17] Sz. Borsanyi et al., Nature **593**, 51 (2021) [arXiv:2002.12347] [Search inSPIRE].
[18] Y. Jho, Y. Kwon, S. C. Park, and P.-Y. Tseng, J. High Energy Phys. **1910**, 168 (2019) [arXiv:1904.13053] [Search inSPIRE].
[19] Y. Jho, S. M. Lee, S. C. Park, Y. Park, and P.-Y. Tseng, J. High Energy Phys. **2004**, 086 (2020) [arXiv:2001.06572] [Search inSPIRE].
[20] K. Ban, Y. Jho, Y. Kwon, S. C. Park, S. Park, and P.-Y. Tseng,J. High Energy Phys. **2104**, 091 (2021) [arXiv:2012.04190] [Search inSPIRE].
[21] m Y. Jho, J.-C. Park, S. C. Park, and P.-Y. Tseng, Phys. Lett. B **811**, 135863 (2020) [arXiv:2006.13910] [Search inSPIRE].
[22] S. C. Park and H. S. Song, Phys. Lett. B **523**, 161 (2001) [arXiv:hep-ph/0109121] [Search inSPIRE].
[23] S. C. Park and H. S. Song, Phys. Lett. B **506**, 99 (2001) [arXiv:hep-ph/0103072] [Search inSPIRE].
[24] S. Kanemura, K. Nishiwaki, H. Okada, Y. Orikasa, S. C. Park, and R. Watanabe, Prog. Theor. Exp. Phys. **2016**, 123B04 (2016) [arXiv:1512.09048] [Search inSPIRE].
[25] B. Zhu and X. Liu,Sci. China-Phys. Mech. Astron. **65**, 231011 (2022) arXiv:2104.03238[Search in SPIRE].
[26] P. Athron, C. Balázs, D. H. J. Jacob, W. Kotlarski, D. Stöckinger, and H. Stöckinger-Kim, J. High Energy Phys. **2109**, 080 (2021) arXiv:2104.03691[Search inSPIRE].
[27] A. Crivellin, D. Müller, and F. Saturnino, J. High Energy Phys. **2006**, 020 (2020) [arXiv:1912.04224] [Search inSPIRE].
[28] M. Lindner, M. Platscher, and F. S. Queiroz, Phys. Rept. **731**, 1 (2018) [arXiv:1610.06587] [Search inSPIRE].
[29] H. Terazawa, Prog. Theor. Phys. **39**, 1326 (1968).
[30] A. Angelescu, D. Bečirević, D. A. Faroughy, and O. Sumensari, J. High Energy Phys. **1810**, 183 (2018) [arXiv:1808.08179] [Search inSPIRE].
[31] D. Buttazzo, A. Greljo, G. Isidori, and D. Marzocca, J. High Energy Phys. **1711**, 044 (2017) [arXiv:1706.07808] [Search inSPIRE].
[32] J. Aebischer, W. Altmannshofer, D. Guadagnoli, M. Reboud, P. Stangl, and D. M. Straub, Eur. Phys. J. C **80**, 252 (2020) [arXiv:1903.10434] [Search inSPIRE].
[33] C. Cornella, J. Fuentes-Martin, and G. Isidori, J. High Energy Phys. **1907**, 168 (2019) [arXiv:1903.11517] [Search inSPIRE].
[34] N. Assad, B. Fornal, and B. Grinstein, Phys. Lett. B **777**, 324 (2018) [arXiv:1708.06350] [Search inSPIRE].
[35] R. Alonso, B. Grinstein, and J. Martin Camalich, J. High Energy Phys. **1510**, 184 (2015) [arXiv:1505.05164] [Search inSPIRE].
[36] L. Calibbi, A. Crivellin, and T. Ota, Phys. Rev. Lett. **115**, 181801 (2015) [arXiv:1506.02661] [Search inSPIRE].
[37] A. Bhaskar, D. Das, T. Mandal, S. Mitra, and C. Neeraj,Phys. Rev. D **104**, 035016 (2021) arXiv:2101.12069[Search inSPIRE].
[38] P. S. Bhupal Dev, R. Mohanta, S. Patra, and S. Sahoo, Phys. Rev. D **102**, 095012 (2020) [arXiv:2004.09464] [Search inSPIRE].

[39] M. Blanke and A. Crivellin, Phys. Rev. Lett. **121**, 011801 (2018) [arXiv:1801.07256] [Search inSPIRE].

[40] A. Crivellin, C. Greub, D. Müller, and F. Saturnino, Phys. Rev. Lett. **122**, 011805 (2019) [arXiv:1807.02068] [Search inSPIRE].

[41] C. Bonilla, T. Modak, R. Srivastava, and J. W. F. Valle, Phys. Rev. D **98**, 095002 (2018) [arXiv:1705.00915] [Search inSPIRE].

[42] R. Alonso, P. Cox, C. Han, and T. T. Yanagida, Phys. Lett. B **774**, 643 (2017) [arXiv:1705.03858] [Search inSPIRE].

[43] B. C. Allanach, Eur. Phys. J. C **81**, 56 (2021); **81**, 321 (2021) [erratum][arXiv:2009.02197] [Search inSPIRE].

[44] M. Du, J. Liang, Z. Liu, and V. Q. Tran, arXiv:2104.05685[Search inSPIRE].

[45] R. L. Workman and Others, Prog. Theor. Exp. Phys. **2022**, 083C01 (2022).

[46] W. J. Marciano, A. Masiero, P. Paradisi, and M. Passera, Phys. Rev. D **94**, 115033 (2016) [arXiv:1607.01022] [Search inSPIRE].

[47] M. Algueró, B. Capdevila, A. Crivellin, S. Descotes-Genon, P. Masjuan, J. Matias, M.-N. Novoa Brunet, and J. Virto, Eur. Phys. J. C **79**, 714 (2019); **80**, 511 (2020) [addendum][arXiv:1903.09578] [Search inSPIRE].

[48] A. G. Akeroyd and C.-H. Chen, Phys. Rev. D **96**, 075011 (2017) [arXiv:1708.04072] [Search inSPIRE].

[49] R. Alonso, B.-N. Grinstein, and J. Martin Camalich, Phys. Rev. Lett. **118**, 081802 (2017) [arXiv:1611.06676] [Search inSPIRE].

[50] M. Blanke, A. Crivellin, S. de Boer, M. Moscati, U. Nierste, I. Nišandžić, and T. Kitahara, Phys. Rev. D **99**, 075006 (2019); [arXiv:1905.08253] [Search inSPIRE].

[51] R. Aaij et al., Phys. Rev. Lett. **118**, 251802 (2017) [arXiv:1703.02508] [Search inSPIRE].

[52] C. Bobeth, M. Gorbahn, T. Hermann, M. Misiak, E. Stamou, and M. Steinhauser, Phys. Rev. Lett. **112**, 101801 (2014) [arXiv:1311.0903] [Search inSPIRE].

[53] W. Altmannshofer, P. Ball, A. Bharucha, A. J. Buras, D. M. Straub, and M. Wick, J. High Energy Phys. **0901**, 019 (2009) [arXiv:0811.1214] [Search inSPIRE].

[54] K. Cheung, C.-W. Chiang, N. G. Deshpande, and J. Jiang, Phys. Lett. B **652**, 285 (2007), hep-ph/0604223.

[55] R. Aaij et al., Phys. Rev. Lett. **123**, 211801 (2019) [arXiv:1905.06614] [Search inSPIRE].

[56] L. Calibbi and G. Signorelli, Riv. Nuovo Cimento **41**, 71 (2018) [arXiv:1709.00294] [Search inSPIRE].

[57] C. McNeile, C. T. H. Davies, E. Follana, K. Hornbostel, and G. P. Lepage, Phys. Rev. D **85**, 031503 (2012) [arXiv:1110.4510] [Search inSPIRE].

[58] J. P. Lees et al., Phys. Rev. Lett. **118**, 031802 (2017) [arXiv:1605.09637] [Search inSPIRE].

[59] J. P. Lees et al., Phys. Rev. D **86**, 012004 (2012) [arXiv:1204.2852] [Search inSPIRE].

[60] D. Bečirević, O. Sumensari, and R. Zukanovich Funchal, Eur. Phys. J. C **76**, 134 (2016) [arXiv:1602.00881] [Search inSPIRE].

[61] Y. Amhis et al., Eur. Phys. J. C **77**, 895 (2017) [arXiv:1612.07233] [Search inSPIRE].

[62] Y. Miyazaki et al., Phys. Lett. B **699**, 251 (2011) [arXiv:1101.0755] [Search inSPIRE].

[63] M. Bordone, C. Cornella, J. Fuentes-Martín, and G. Isidori, J. High Energy Phys. **1810**, 148 (2018) [arXiv:1805.09328] [Search inSPIRE].

[64] C. Hati, J. Kriewald, J. Orloff, and A. M. Teixeira, J. High Energy Phys. **1912**, 006 (2019) [arXiv:1907.05511] [Search inSPIRE].

[65] B. Bhattacharya, A. Datta, J.-P. Guévin, D. London, and R. Watanabe, J. High Energy Phys. **1701**, 015 (2017) [arXiv:1609.09078] [Search inSPIRE].

[66] W. Altmannshofer, S. Gori, M. Pospelov, and I. Yavin, Phys. Rev. Lett. **113**, 091801 (2014) [arXiv:1406.2332] [Search inSPIRE].

[67] L. Di Luzio, M. Kirk, A. Lenz, and T. Rauh, J. High Energy Phys. **12**, 009 (2019) [arXiv:1909.11087] [Search inSPIRE].

[68] A. J. Buras and R. Fleischer, in Heavy Flavours II (World Scientific, Singapore, 1998), Advanced Series on Directions in High Energy Physics, Vol. 15, p. 65[arXiv:hep-ph/9704376] [Search inSPIRE].

[69] F. Pandolfi, arXiv:1709.06119[Search inSPIRE].

[70] A. M. Sirunyan et al., J. High Energy Phys. **1803**, 166 (2018) [arXiv:1709.05406] [Search inSPIRE].

[71] A. M. Sirunyan et al., J. High Energy Phys. **2107**, 208 (2021) [arXiv:2103.02708] [Search inSPIRE].
[72] Y. Amhis et al., Eur. Phys. J. C **77**, 895 (2017) [arXiv:1612.07233] [Search inSPIRE].
[73] Y. Amhis et al., arXiv:2206.07501[Search inSPIRE].
[74] W. Altmannshofer and P. Stangl, Eur. Phys. J. C **81**, 952 (2021) [arXiv:2103.13370] [Search inSPIRE].
[75] G. D'Ambrosio, A. M. Iyer, F. Mahmoudi, and S. Neshatpour, J. High Energy Phys. **2209**, 148 (2022) [arXiv:2206.14748] [Search inSPIRE].
[76] M. Endo, T. Kitahara, S. Mishima, and K. Yamamoto, Phys. Lett. B **771**, 37 (2017) [arXiv:1612.08839] [Search inSPIRE].